

VORTEX MOVEMENT AND MAGNETIZATION OF HIGH T_c SUPERCONDUCTORS

A.L. Roytburd and M.J. Turchinskaya*

Engineering Materials Program

Department of Chemical and Nuclear Engineering, University of Maryland

College Park, MD 20742-2111

*Metallurgical Division, NIST, Gaithersburg, MD 20899

ABSTRACT

The basic characteristics of the thermoactivated vortex mobility in $Y_1Ba_2Cu_3O_7$ are determined by measurement of the kinetics of magnetization in two time regimes. The analysis of the kinetics of the approach of the equilibrium results in the activation energy, while the measurement of the log-creep rate allows determination of the activated moment. It is shown that the movement of vortices can be regarded as the diffusion process.

INTRODUCTION

The problem of vortex pinning is of great importance for the application of oxide high T_c superconductors. In comparison with pinning of dislocations, interface boundaries or domain walls, the pinning problem for vortices is much more complex because the density of vortices is large and adequate to produce strong interactions between the vortices in many practical important cases.

In accordance with the effects of vortex-vortex interactions on pinning two different cases can be considered. The first one corresponds to strong pinning centers with the spacing much larger than the distance between vortices. In this case the system of vortices can be considered an equilibrium phase (crystal, glass or melt), and the interaction of this phase with randomly distributed pinning obstacles can be analyzed. A classic example of such an approach is the Labusch theory of pinning for an elastic vortex lattice.¹ Another example is Nelson's melt theory,² which pretends to the explanation of the very weak pinning at temperatures above the reversibility temperature. Note that before melting, a great number of dislocations must be formed in the vortex crystal, and the real problem of the dynamics of the vortex medium in this case is the problem of movement and pinning of dislocations in the vortex lattice. In other words the trend to melting has to be manifested by a transition from a laminar flow of the vortex medium to a turbulent one. This problem seems very important in the case of pinning by interfaces or particles with spacing larger than a distance between vortices.³

However, the problem of intrinsic pinning in oxide superconductors may be closer to reality in the other case, where the individual vortices are pinned by the obstacles, and the distance between the obstacles is comparable with the distance between vortices. Collective effects of the vortex-vortex interactions are important in this case also, but we can expect that they manifest themselves in the renormalization of parameter values rather than in the alteration of the physical picture of the vortex motion. This case of small vortex density is under consideration in the paper. Our goal is to obtain basic characteristics of vortex mobility from the study of the magnetization of zero-field cooled samples.

THEORETICAL CONSIDERATION

The penetration of magnetic flow into a superconductor during its magnetization in an external magnetic field, Fig. 1, is similar to the flux flow diffusion,^{4,5} and is described by the generalized diffusion equation:

$$\partial B / \partial t = \nabla (D_{\text{eff}} \nabla B), \quad (1)$$

where $D_{\text{eff}} = vB / \nabla B$ is the effective flux diffusion coefficient, B is the local induction, ∇B is the gradient of the induction, and v is the flux velocity.

The equation (1) is correct if there is no nucleation, multiplication or annihilation of vortices inside the sample, i.e. there are no weak links within a superconductor. The flux velocity for the thermoactivated movement of a vortex through an array of pinning obstacles can be determined as

$$v = v_0 \exp(-U/kT) \sinh(\alpha \nabla B / kT). \quad (2)$$

This equation is obtained under the assumption that the energy barrier ΔF , which has been overcome for a vortex displacement, is disturbed under the driving force (∇B), and it is an analytical function of ∇B at $\nabla B = 0$.^{4,6}

$$\Delta F^\pm(\nabla B) = \Delta F(0) \mp \alpha \nabla B, \quad \Delta F(0) = U, \quad (3)$$

where $+$ corresponds to displacements with ∇B , $-$ to the opposite direction, U is the activation energy, and α is the activated moment. $\alpha = m l_1$, $m = \phi_0 n l_2$, where m is the magnetic moment of the vortex or vortex bundle, $\phi_0 = 2.7 \times 10^{-7} \text{ Gcm}^2$ is the flux of one vortex, n is the number of the vortices in the bundle, l_1 is the displacement of the bundle or vortex at an activation event, l_2 is the effective length of a displaced section of the bundle or vortex, factually the distance between the nearest pinning points along the vortex, (Fig. 2). v_0 in Eq. (2) is the limiting velocity which equals $l_1 \nu$, where ν is the frequency of vibration of the vortex section, l_2 . Assuming $\nu \sim (\xi / l_2) \nu_{\text{at}}$, where ξ is the coherence length or vortex "radius" ($\sim 10^{-8} \text{ cm}$), ν_{at} is the atomic vibration frequency $\sim 10^{13} \text{ s}^{-1}$, we get for $v_0 \approx \xi \nu_{\text{at}} \approx 10^5 \text{ cm/s}$, a value on the order of the sound velocity.

If the driving force is larger than the critical force, $\nabla B > \nabla B_{\text{cr}} = U/\alpha$, the movement of the vortex is overbarrier. The vortex movement is not described by Eq. (2) because it is controlled not by the frequency of fluctuation depinning events but by the rate of the dissipation of the vortex energy. In this case $v = (1/\gamma) \nabla B$, where γ is the viscosity.^{7,8}

The vortex velocity, $v(\nabla B)$, and the corresponding diffusion coefficient, $D_{\text{eff}}(\nabla B)$, are given in Fig. 3. There are three regions for which the solution of Eq. (1) can be obtained analytically.

The first one corresponds to the distribution of magnetic induction with $\nabla B > \nabla B_{\text{cr}}$. This is the so called flux flow region when $D_{\text{eff}} = D_f = B/\gamma$ is independent on ∇B .

The second region corresponds to the near critical state, when $\alpha \nabla B / kT \gg 1$, and $\sinh(\alpha \nabla B / kT) \approx \exp(\alpha \nabla B / kT)$. In this region the total magnetization of a superconductor, or its average induction, is proportional to the logarithm of

time:^{4,6}

$$M(t) \approx P \ln t, \quad P = dM/d \ln t \approx kTR/(\partial \Delta F / \partial VB) = (kTR/\alpha(R)), \quad (4)$$

where R is the radius of the sample, $\alpha(R)$ is the activated moment at its surface, where the induction $B(R)$ is closed to the equilibrium one, B_0 .

The third region corresponds to the constant $D_{eff}=D$ at the small VB again:

$$D = (B_0 \alpha v_0 / kT) \exp(-U/kT) = D_0 \exp(-U/kT), \quad D_0 = B_0 \alpha v_0 / kT \quad (5)$$

This regime of ordinary diffusion flow was named the thermally assisted flux flow (TAFF).⁸

It is important to note, that all of these regimes can be observed by measuring the magnetization as a function of time of the zero-field cooled superconductor sample. At the first moment after applying the magnetic field, VB is great and is larger than the critical value. Unfortunately, this stage is difficult to study because of nonstationary effects while the field is turned on. The sample then goes through the near critical state, where linear behaviour of magnetization vs. logarithm of time has been expected. At last, in the final stage, the magnetization approaches to the equilibrium saturation, M_0 (or B_0), at $t > t^*$, and the kinetics of the magnetization is described by the equation:

$$M(t) = M_0 + M' \exp(-t/\tau), \quad (6)$$

where M' is a constant. The relaxation time, τ , is connected with the diffusion coefficient, $D(B_0)$, by the relation $\tau = R^2/D$, where R is the sample radius. It is necessary to stress that this near equilibrium asymptotic behaviour does not depend on the distribution of the local induction at the moment t^* , when the exponential stage begins, provided the induction is closed to B_0 ($VB/B_0 \ll 1$).

Thus the study of the kinetics of the magnetization at the different stages gives the opportunity to find the basic characteristics of the vortex mobility, α and U , without any additional assumption about the distribution of the induction within the sample. The results of such a kind of study are represented below.

SAMPLES AND EXPERIMENTAL METHOD

Three different $Y_1Ba_2Cu_3O_7$ samples with sharp transitions at $T_c=93K$ were under investigation: a single crystal, a sintered polycrystal and a sample of quench, melt and growth (QMG) material.¹⁰ The QMG sample is a bar of $0.9 \times 0.9 \times 5.8$ mm, which was cut from a grain of a polycrystal. The sample has no weak links,¹¹ making it possible to determine its effective radius, R ($R \approx 0.45$ mm). Our single crystal sample contains some fraction of normal phase. So, the single crystal as well as sintered samples were not good for quantitative estimates.

The samples were cooled in zero magnetic field. The magnetic field was then applied, and the magnetization was measured as a function of time using either a vibrating sample magnetometer, (VSM), or a SQUID system. The magnetic field was directed along c axes of the single crystal sample and perpendicularly to c axes of the QMG sample.

EXPERIMENTAL RESULTS

Approach to Equilibrium Magnetization, M_0 , Diffusion Coefficient, D . Magnetization versus time, $M(t)$, curves were measured at rather high temperatures (70 and 80K) and for long exposures (up to 340 ksec) at relatively weak magnetic fields (2 and 4 kOe), so the density of vortices was small up to approaching the equilibrium magnetization. $M(t)$ data for all the samples at 70K and 2 kOe are plotted in curves (a) of Figures 4, 5 and 6 for the QMG, single crystal and sintered samples, respectively. M vs. log-time data are plotted in curves (b). Curves obtained for the other temperature and field setting have the same shape as in these Figures: for all the curves there are log-time dependences $M(t)$, and at much longer times, $t > t^*$ there are stages of the approach to the equilibrium magnetization, M_0 . In these stages the magnetization shows the exponential behaviour:

$$\ln[M(t)/M_0 - 1] - \ln(M'/M_0) = -t/\tau, \quad (7)$$

where $\ln(M'/M_0)$ are constants. In curves (c) of Fig. 4, 5 and 6, where the calculated data of $\ln[M(t)/M_0 - 1]$ vs. time for all the samples are plotted, it can be seen that at $t > t^*$ there are linear dependences of $\ln[M(t)/M_0 - 1]$ on time. The result of the determination of τ depends strongly on the chosen value of M_0 , and a special asymptotic method was used¹² for the correction the values of M_0 . For the QMG sample we obtained the values of $M_0 = -3.87$ (emu/gr) at 70K and 2 kOe, and $M_0 = -2.5$ (emu/gr) at 70K and 4 kOe.

The values of the relaxation time, τ , were obtained as a slope of the linear portion of the curves (c), and the diffusion coefficients, $D = R^2/\tau$, where R is the effective radius of the sample, were calculated. For the QMG sample at 70K we obtained $D = 6.7 \times 10^{-9}$ cm²/s for 2 kOe, and $D = 7.8 \times 10^{-9}$ cm²/s for 4 kOe.

Activated Moment, α , Activated Length, ℓ , and Intervortex Spacing, a . The logarithmic creep rate $P = dM/d \ln t$ for the QMG and sintered samples was measured in the temperature interval 6-80K.¹⁰ The results are given in Fig. 7, a and in Fig. 7, b, respectively. For the QMG sample we calculated the values of the activated moment, α (using the relation $\alpha = kTR/P$, Eq. (4)). Derived values of α/ϕ_0 , where ϕ_0 is the flux of one vortex, for the QMG sample are plotted in Fig. 8.

Values of the average activated length, $\ell = (\alpha/\phi_0)^{1/2}$, are displayed in Fig. 9 together with values of the distance between vortices, $a = (B_0/\phi_0)^{1/2}$. B_0 was obtained from measuring the equilibrium magnetization, M_0 : $B_0 = 4\pi M_0 + H$.

Activation Energy, U , and Pre-exponential Factor, D_0 . Obtaining τ and α from the kinetics of the magnetization, it is possible to estimate the activation energy of the thermoactivated movement of the vortex bundle, U , from the Eq. (5):

$$U/kT = \ln(D/D_0) = \ln(\tau v_0 B_0 \alpha / kTR^2). \quad (8)$$

Assuming that $v_0 = 10^5$ cm/s, we obtained, with log-accuracy by v_0 , $U/kT \approx 33$, $U \approx 0.19$ eV, and the pre-exponential factor $D_0 = B_0 \alpha v_0 / kT \approx 6 \times 10^5$ cm²/s for the QMG sample at 70K and 2 kOe. For 70K and 4 kOe $U \approx 0.2$ eV, $D_0 \approx 4 \times 10^6$ cm²/s.

DISCUSSION

The exponential approach to equilibrium is evidence of the linear dependence between the vortex velocity and the driving force and supports the assumption of Eq. (3). Taking into account the relation between D_{eff} and resistance, $\rho : \rho = D/c^2$, where c is the velocity of light, we have to admit that at 70 and 80K and $H=2$ and 4 kOe the QMG sample of $YBa_2Cu_3O_7$ manifests small but finite resistivity. From the point of view of vortex mobility in this stage, the vortex medium is rather "melt" than "glass" (in terms of M.Fisher's theory¹³) or "crystal" with collective pinning.¹⁴ For both these models ΔF must be the divergent function of ∇B at $\nabla \rightarrow 0$: $\Delta F \sim 1/\nabla B^\beta$, $\beta > 0$ for the vortex glass state, or $\sim \ln \nabla B$ for the collective pinning model.

By "vortex melt", we imply that the effects of correlations between the individual thermoactivated depinning events are small.¹⁵ To prove this suggestion it is necessary to consider the pre-exponential factor, D_0 , in Eq. (5) in more detail, rewriting it through the activated length, ℓ , and the intervortex distance, a , as

$$D_0 = (\phi_0^2/kT)(\ell^2/a^2)v_0 = Lv_0(\ell^2/a^2). \quad (9)$$

The term, $\phi_0^2/kT = L$, has the dimension of length (e.g. $L \approx 4$ cm at 70K). From Fig. 10 it is clear that up to 70K at 2 kOe and 60K at 4 kOe, $\ell < a$, i.e. a bundle consists of only one vortex, and ℓ is the weak function of temperature. Then ℓ rises rapidly, i.e. the number of vortices in the bundle increases. For $n=1$, $\ell = (\ell_1 \ell_2)^{1/2}$, that is, ℓ is close to an average distance between pinning points.

At 70K and higher temperatures, all the pinning centers are occupied by vortices, and the pinning-depinning movements of vortices with the driving force ∇B can be interpreted as back-directed diffusion of pinning points in vortex medium. Indeed, the velocity of the point flow is determined by the Einstein diffusion relation:

$$v_p = (D_p/kT)\nabla\mu \approx (D_p/kT)(\alpha\nabla B/a), \quad (10)$$

where $D_p = a^2 \nu \exp(-U/kT)$ is the point diffusion coefficient, and $\nabla\mu$ is the gradient of chemical potential of the pinning points in the magnetic field. The point velocity, v_p , is equal numerically to the vortex velocity, v :

$$-v_p = v = D\nabla B/B \quad (11)$$

(the relation between D and v arises from the definition of D_{eff} in Eq. (1)). If we take into account that $a\nu = v_0$, it follows from Eqs. (10) and (11) that the vortex diffusion coefficient, D , is determined by Eq. (5). At $\ell \approx a$, $D_0 \approx Lv_0 \approx 10^6 \text{ cm}^2/\text{s}$: that is in accordance with the experimental determination of D_0 through measuring α and B_0 .

It is clear that the penetration of the flux flow into a sample during magnetization can be considered in terms of the diffusion theory for polycrystal samples with weak grain boundaries too. For this case it would be necessary to bring into consideration the vortex diffusion along the grain boundaries as well as the bulk grain diffusion. Of course the diffusion description may be not

complete if the nucleation of vortices is possible inside "bad" samples.

CONCLUSION

1. It is shown that approach to equilibrium magnetization with time of the zero-field cooled QMG, single crystal and sintered samples of $\text{YBa}_2\text{Cu}_3\text{O}_7$, proceeds according to the exponential law. The equilibrium values of the induction, relaxation time and vortex diffusion coefficient are determined for the QMG sample at 70 and 80K and 2 and 4 kOe.
2. Log-creep rate was measured at 2 and 4 kOe for a set of temperatures between 6 and 80K. From these data the activated moment α was found. The analysis of α shows that an activated vortex bundle contains only one vortex at the temperatures and fields under consideration. An activation length, $l = (\alpha/\phi_0)^{1/2}$, is almost constant up to 70 or 80 K. Beyond these temperatures the distance between vortices becomes smaller than l . Up to these temperatures l is likely the average distance between effective pinning points. At temperatures higher than 70K at field 2 kOe and temperatures $\sim 75\text{K}$ at 4 kOe the number of vortices in a bundle grows, as does l .
3. Using B_0 and D , which are obtained from the approach to the equilibrium, and α from the log-creep stage, the activation energy, U , has been determined for the QMG sample.
4. The character of vortex movement during magnetization with time at 70 and 80K and 2 and 4 kOe is in good agreement with the diffusion picture, which does not take into account the effects due to the correlation between individual thermoactivation events.

ACKNOWLEDGEMENT

We are very grateful to L.H. Bennet and L.J. Swartzendruber for their friendly collaboration and to K. Sawano, D.L. Kaiser, J.E. Blendell, and C.K. Chiang for the samples.

REFERENCES

1. R. Labusch, Phys. Stat. Sol. 32, 439 (1967), Crystal Lattice Defects 1, 1 (1969).
2. D.R. Nelson and H.S. Seung, Phys. Rev. B39, 9153 (1989).
3. M.J. Turchinskaya and A.L. Roytburd, JETP Lett. 20, 79 (1974).
4. M.R. Beasley, R. Labusch, W.W. Webb, Phys. Rev. 181, 681 (1969).
5. E.M. Brandt, Z. Physik B., in press.
6. P.W. Anderson, Phys. Rev. Lett., 9, 309 (1962).
7. M. Tinkham, Phys. Rev. Lett., 13, 804 (1964).
8. L. Bardeen and M.J. Stephen, Phys. Rev. 140, A1197 (1965).
9. P.H. Kes, J. Aarts, J. van der Berg, and J.A. Mydosh, Supercond. Sci. Technol., 1, 242, (1989).
10. M.J. Turchinskaya, L.H. Bennet, L.J. Swartzendruber, A. Roytburd, C.K. Chiang, M. Hill, J.E. Blendell, and K. Sawano, High-Temperature Superconductors: Fundamental Properties and Novel Materials Processing. MRS Symp. Proc. 169, in press, (1990).
11. M. Murakami, M. Morita, and N. Koyama, Jpn. J. Appl. Phys., 28, L1125 (1989).
12. M.J. Turchinskaya, A.L. Roytburd, L.H. Bennett, L.J. Swartzendruber, and K.

Sawano, in preparation.

13. M.P.A. Fisher, Phys. Rev. Lett., 62, 1425 (1989).
14. M.V. Feigelman, V.B. Geshkenbain, A.L. Larkin, and V.M. Vinocur, Phys. Rev. Lett., 63, 2303 (1989).
15. A.L. Roytburd, M.J. Turchinskaya, L.H. Bennett, and L.J. Swartzendruber, submitted for publication.

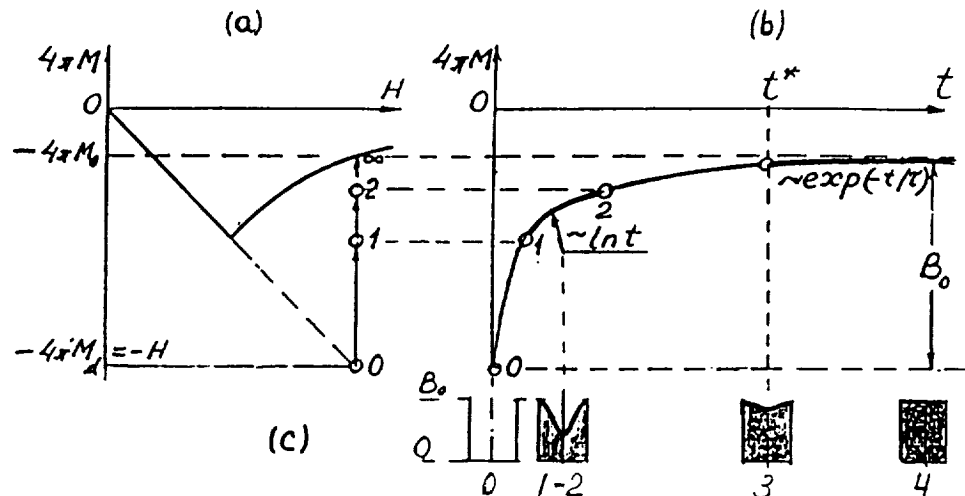


Fig. 1. Kinetics of magnetization of a zero-field cooled sample.
a. Equilibrium magnetization dependence on magnetic field.
b. Time dependence of magnetization.
c. Distribution of magnetic induction.
0 - the initial diamagnetic state, 1-2 - the near critical state ($\nabla B \leq \nabla B_{cr}$),
3 - the near equilibrium state, 4 - the equilibrium state ($\nabla B = 0$, $B = B_0$).

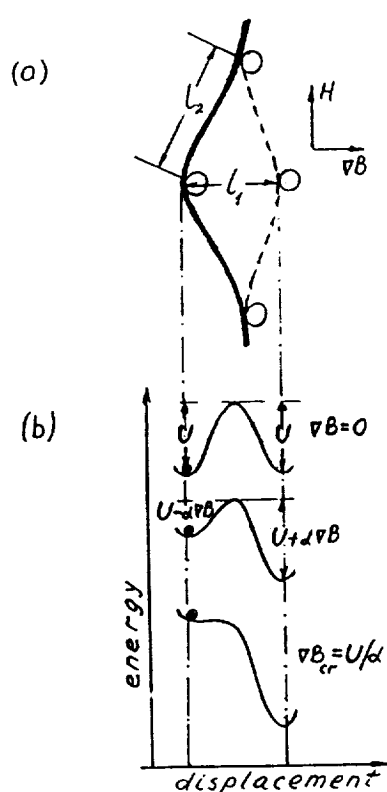


Fig. 2.

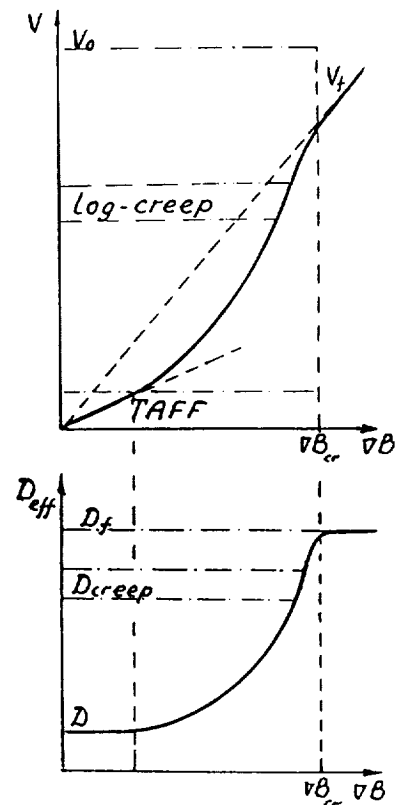


Fig. 3.

Fig. 2. Thermoactivated movement of a vortex. a. A vortex section, l_2 , pinned by obstacles, b. Energy as function of a vortex displacement.
Fig. 3. Vortex velocity, v , and vortex diffusion coefficient, D_{eff} .

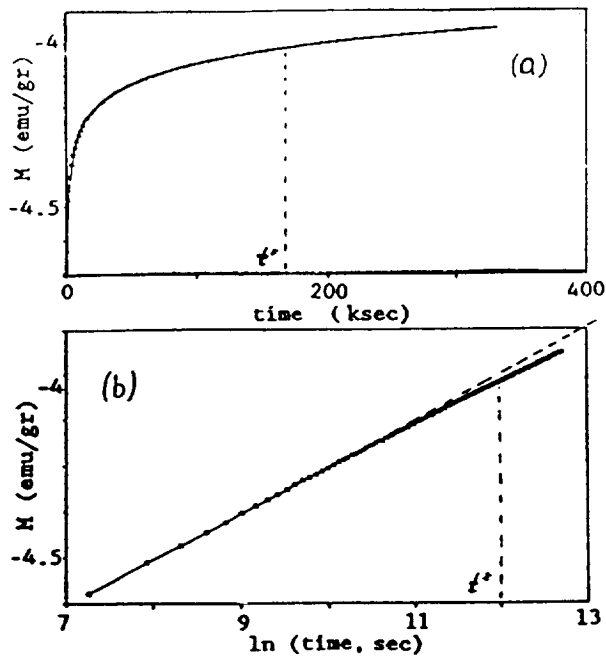


Fig. 4.

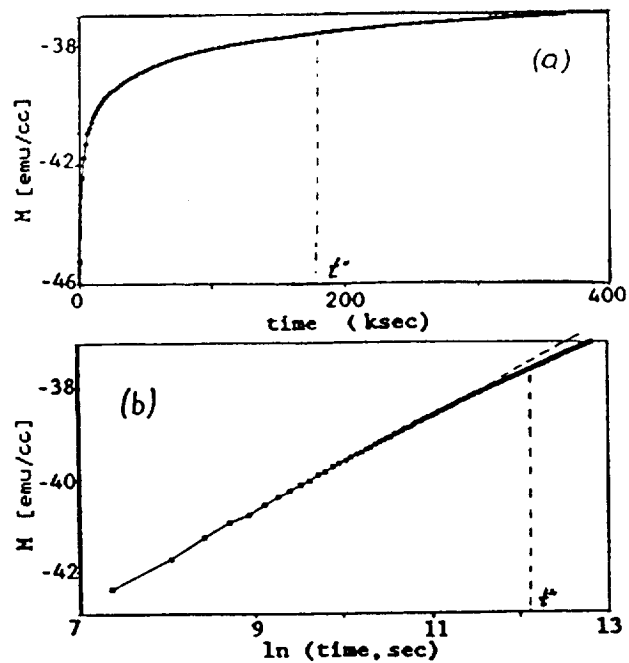


Fig. 5.

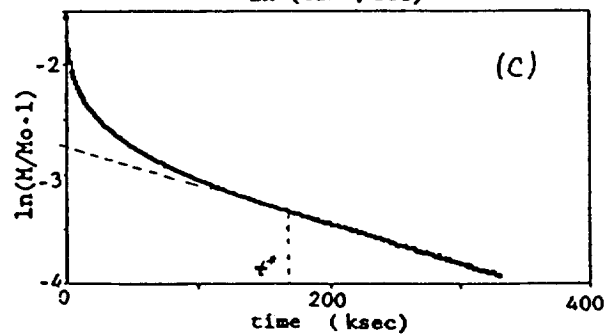


Fig. 6.

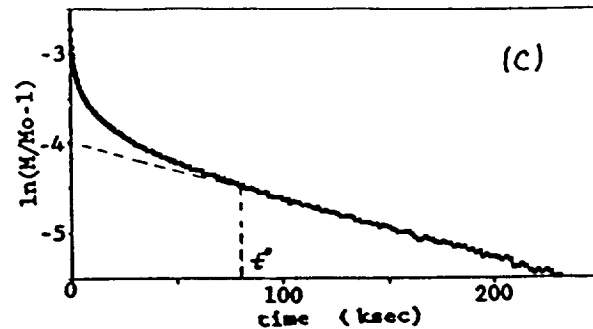
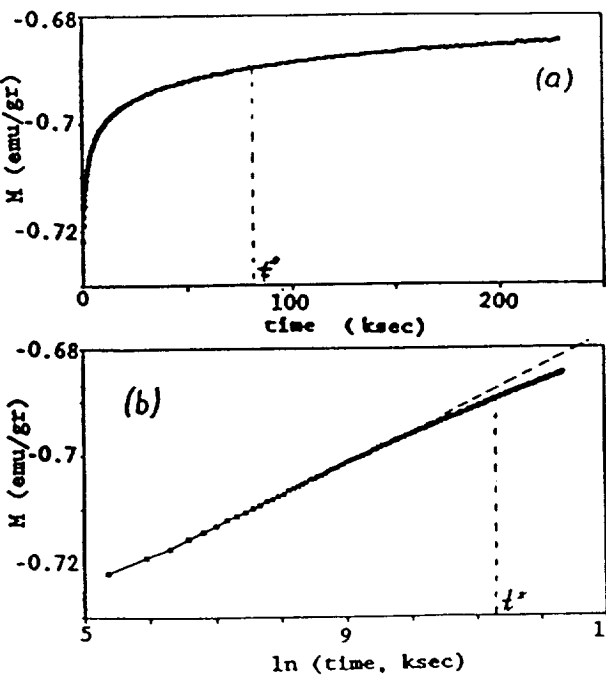


Fig. 4. Kinetics of magnetization of the QMG sample, $M_0 = -3.87$ (emu/gr).
 Fig. 5. Kinetics of magnetization of the single crystal sample, $M_0 = -36.25$ [emu/cc].
 Fig. 6. Kinetics of magnetization of the sintered sample, $M_0 = -0.68$ (emu/gr).

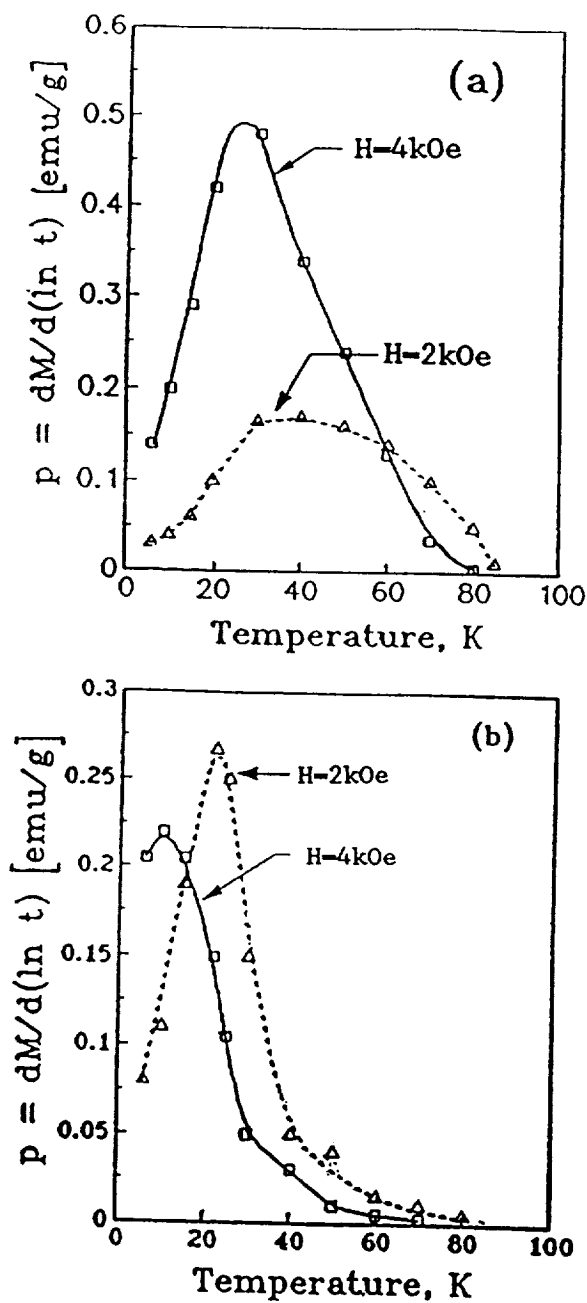


Fig. 7.

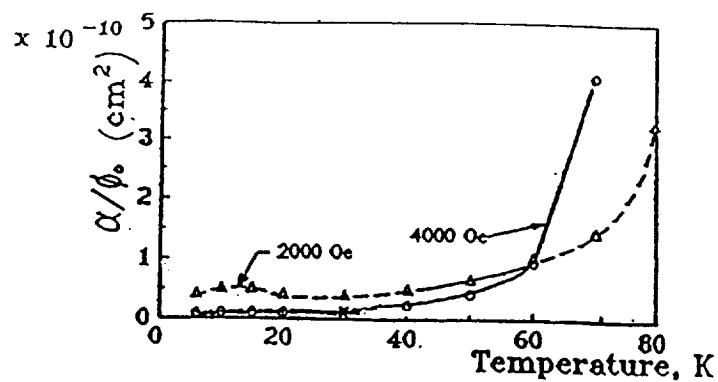


Fig. 8.

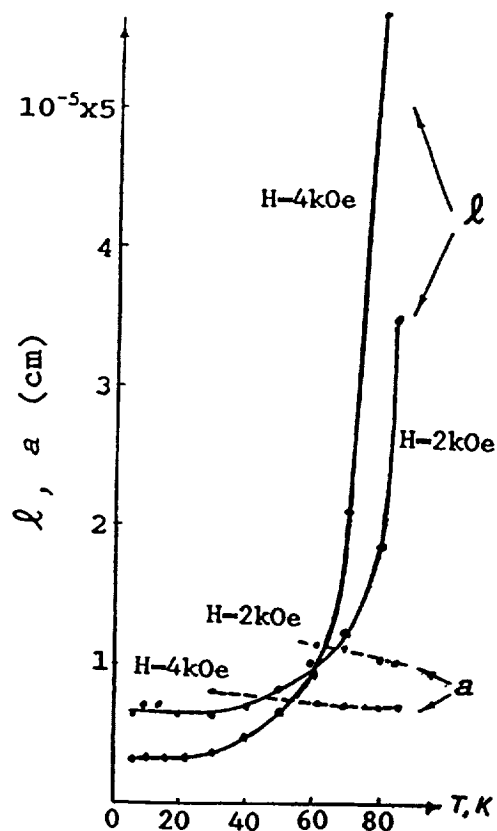


Fig. 9.

Fig. 7. Logarithmic rate of magnetization, P .

a. the QMG sample, b. the sintered sample.

Fig. 8. Temperature dependence of α/ϕ_0 for the QMG sample at 2 and 4 kOe.

Fig. 9. Temperature dependence of average activated length, ℓ , and intervortex spacing, a , for the QMG sample at 2 and 4 kOe.